DFT-Spread Spectrally Efficient Non-Orthogonal FDMA

(Invited Paper)

Tongyang Xu and Izzat Darwazeh

Department of Electronic and Electrical Engineering, University College London, London, UK
Email: tongyang.xu.11@ucl.ac.uk, i.darwazeh@ucl.ac.uk

***Abstract*—Single carrier frequency division multiple access (SC-FDMA) has been comprehensively investigated and standardized in 4th generation (4G) and 5th generation (5G) mobile systems. Its significant advantage is low peak-to-average power ratio (PAPR), which makes it suitable for uplink channel communications. However, over a long time period, SC-FDMA has not made breakthrough especially in data rate enhancement, which may not catch up with the next generation evolution in communications. This work proposes to use a non-orthogonal waveform in SC-FDMA to promote a new concept, termed single carrier spectrally efficient frequency division multiple access (SC-SEFDMA). This non-orthogonal single carrier access technique maintains essentially similar complexity as SC-FDMA but advantageously can either achieve higher data rate for the same amount of power consumption or the same data rate with less power consumption.**

***Index Terms*—Single carrier, non-orthogonal, SEFDM, SC-SEFDMA, SC-FDMA, OFDMA, PAPR, LDPC.**

I. Introduction

The traditional orthogonal frequency division multiple access (OFDMA) [1] access technique has the benefits in immunity to multipath fading and inter-symbol interference, but at the cost of high peak-to-average power ratio (PAPR) due to multiple sub-carriers overlapping. Therefore, a more complex power amplifier is required to guarantee signal linearity below the saturation point, which results in low power efficiency and high cost. An alternative solution is its single carrier format, which is termed single carrier frequency division multiple access (SC-FDMA) [2]. Since SC-FDMA spreads a narrow band signal on a wider band of multiple sub-carriers, its characteristic becomes similar to a single carrier signal and therefore has lower PAPR [3].

There are two sub-carrier mapping schemes for SC-FDMA signals; distributed sub-carrier mapping and localized sub-carrier mapping [2]. The distributed sub-carrier mapping is referred to distributed FDMA (DFDMA), which allocates sub-carriers sparsely over the entire signal band. The localized sub-carrier mapping is referred to localized FDMA (LFDMA), which occupies consecutive sub-carriers. The difference between the two schemes is apparent in that DFDMA achieves frequency diversity at the cost of occupying the entire signal bandwidth while LFDMA makes better use of signal bandwidth by densely packing sub-carriers at the expense of weaker frequency diversity. This work will focus on the LFDMA since signal bandwidth is more efficiently used.

978-1-7281-2625-8/19/$31.00 © 2019 IEEE

Traditional SC-FDMA follows the orthogonality principle, where different users are allocated on orthogonally packed sub-carriers. In this case, inter-user interference is avoided. However, with the increased demand for higher spectral efficiency, orthogonal-based resources may no longer be sufficient. This pushes for the use of non-orthogonal resources, which would dramatically improves spectral efficiency.

This work will first explain a non-orthogonal multicarrier signal waveform, termed spectrally efficient frequency division multiplexing (SEFDM) [4], which can increase spectral efficiency by compressing sub-carrier spacing while maintaining the same sub-carrier bandwidth. Its applications in spectrally efficient frequency division multiple access (SEFDMA) and single carrier spectrally efficient frequency division multiple access (SC-SEFDMA) are explored with evaluations of PAPR and effective data rate. The detection of non-orthogonal SEFDM signals has been explored using model based algorithms in [5], [6] or machine learning based approach in [7]. Both detection strategies aim to mitigate the inter carrier interference (ICI) but at the cost of either computational complexity or performance degradation. This work will skip tailored and complex signal detectors and apply the simple matched filter (MF) to recover signals. The mitigation of the self-created ICI is managed by the 5G new radio (NR) defined low density parity check (LDPC) channel coding [8], [9]. Results show the superiority of SC-SEFDMA over SC-FDMA in achieving lower PAPR and higher data rates.

II. Signal Model

This section will first explain the principle of non-orthogonal SEFDM signals. Then the non-orthogonal concept will be applied in single carrier access scenarios.

A. SEFDM Waveform

The principle of an orthogonal frequency division multiplexing (OFDM) signal waveform is illustrated in Fig. 1 where 12 sub-carriers are orthogonally packed without ICI. Two types of SEFDM signals are introduced in Fig. 1. In the SEFDM Type-I waveform, the same number of sub-carriers is used but with closer sub-carrier spacing. In this case, ICI is introduced while spectral bandwidth resource is saved. This

gives us a vision that achieving the same data rate, SEFDM occupies only a portion of the OFDM signal bandwidth. For the SEFDM Type-II waveform, the occupied signal bandwidth is similar to the OFDM waveform but with wider sub-carrier bandwidth. In this case, the data rate of SEFDM Type-II waveform is higher than that of OFDM signals over the a given bandwidth occupation. Two types of SEFDM signals are used according to specific scenarios.

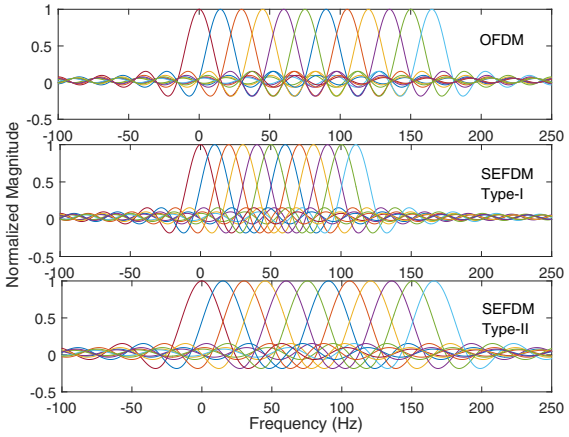

Fig. 1. Sub-carrier allocation schemes for different multicarrier signals. OFDM (12 sub-carriers, data rate is R_b). SEFDM Type-I (12 sub-carriers, bandwidth compression factor α, data rate is R_b). SEFDM Type-II (12 sub-carriers, bandwidth compression factor α, data rate is R_b/α).

The discrete SEFDM signal $X[k]$ is given by

$$X[k] = \frac{1}{\sqrt{N}} \sum_{n=0}^{N-1} s_n \exp\left(\frac{j2\pi nk\alpha}{N}\right), \tag{1}$$

where $\alpha = \Delta f T$ is the bandwidth compression factor, Δf denotes the sub-carrier spacing and T is the period of one SEFDM symbol. N is the number of sub-carriers, $X[k]$ is the k^{th} time sample with $k = [0, 1, ..., N-1]$, s_n is a QAM symbol modulated on the n^{th} sub-carrier and $\frac{1}{\sqrt{N}}$ is a scaling factor for power normalization. The percentage of bandwidth saving is equal to $(1-\alpha) \times 100\%$. For OFDM signals $\alpha = 1$, and $\alpha < 1$ for SEFDM.

B. SEFDM Signal Generation

A standard inverse fast Fourier transform (IFFT) is applicable to OFDM signal generation due to sub-carrier orthogonality. In order to use the IFFT algorithm for SEFDM signals, two modified algorithms are specially designed for SEFDM. Either using a single IFFT or multiple IFFTs [10].

1) Single IFFT: A straightforward way is to pad zeros at the end of each input vector (i.e. a vector consists of N QAM symbols). Therefore, the length of an original IDFT becomes $M = N/\alpha$ where QAM symbols are appended to the first N inputs and zeros are appended to the last $M - N$ remaining inputs as the following

$$s_i^{'} = \begin{cases} s_i & 0 \leq i < N \\ 0 & N \leq i < M \end{cases}, \tag{2}$$

where the value of N/α has to be an integer and simultaneously a power of two, $N/\alpha \in 2^{(\mathbb{N}_{>0})}$, which allows the IDFT to be implemented by the computationally efficient radix-2 IFFT. The SEFDM signal in a new format is expressed as

$$X^{'}[k] = \frac{1}{\sqrt{M}} \sum_{n=0}^{M-1} s_n^{'} \exp\left(\frac{j2\pi nk}{M}\right), \tag{3}$$

where $n, k = [0, 1, ..., M-1]$. The output is truncated with only N samples reserved and the rest $M - N$ samples are discarded.

2) Multiple IFFTs: The limitation of the first method is the requirement of $N/\alpha \in 2^{(\mathbb{N}_{>0})}$. This section explains a multiple IFFTs architecture, which can relax the choice of N and α. Unlike the zero padding at the end of each QAM vector, the multiple IFFTs algorithm interpolate zeros across the entire QAM vector. Assume $\alpha = b/c$, where b and c are both positive integers (i.e. $b, c \in \mathbb{N}_{>0}$) and $b < c$, the interpolated vector becomes a longer version of cN length. By a proper vector rearrangement, the cN length vector can be transformed to c parallel data streams and each has N symbols. In this case, an N-point IFFT can be employed for each stream. The vector rearrangement is expressed in the following

$$X[k] = \frac{1}{\sqrt{N}} \sum_{n=0}^{cN-1} s^{'}(n) \exp\left(\frac{j2\pi nk}{cN}\right), \tag{4}$$

where $s^{'}$ is a cN-dimensional vector of symbols as

$$s^{'}(i) = \begin{cases} s_{i/b} & i \ mod \ b = 0 \\ 0 & otherwise \end{cases}. \tag{5}$$

Equation (4) can further be modified by substituting with $n = i + lc$

$$X[k] = \frac{1}{\sqrt{N}} \sum_{i=0}^{c-1} \sum_{l=0}^{N-1} s^{'}(i + lc) \exp\left(\frac{j2\pi k(i + lc)}{cN}\right). \tag{6}$$

With further rearrangement, (6) is expressed as

$$X[k] = \frac{1}{\sqrt{N}} \sum_{i=0}^{c-1} \exp\left(\frac{j2\pi ik}{cN}\right) \sum_{l=0}^{N-1} s^{'}(i+lc) \exp\left(\frac{j2\pi lk}{N}\right). \tag{7}$$

The new expression reveals that the SEFDM signal generation is equivalent to a combination of c parallel IFFT operations each of N points. The first term on the right hand side of (7) indicates a phase offset operation for each IFFT stream, while the second term is a traditional N-point IFFT operation.

C. Single Carrier SEFDMA

The principles of SC-FDMA and SC-SEFDMA are presented in Fig. 2(a) and Fig. 2(b), respectively. The two block diagrams have the similar system architectures except that SC-SEFDMA employes M-point inverse discrete fractional Fourier transform (IDFrFT) [11] at the transmitter and M-point discrete fractional Fourier transform (DFrFT) at the receiver. The signal processing of IDFrFT and DFrFT can

be simplified using IFFT and FFT according to the previous analysis in Section II-B. The N-point DFT and N-point IDFT are also replaceable by FFT and IFFT, respectively. There are different strategies of sub-carrier mapping [2] such as localized and distributed approaches. Both mapping schemes are applicable to SC-FDMA and SC-SEFDMA.

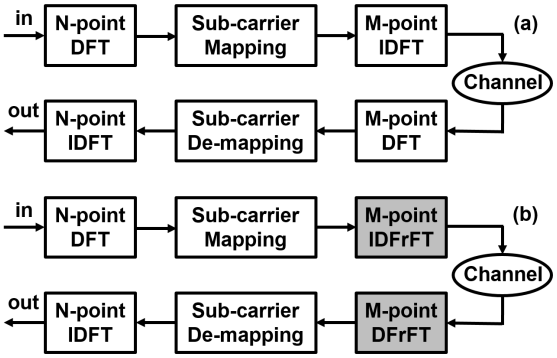

Fig. 2. Transmitter and receiver architectures for SC-FDMA and SC-SEFDMA systems.

III. Performance Comparison

The main advantage of single carrier FDMA/SEFDMA is low PAPR. The cumulative distribution function (CDF) is widely used to measure the probability of PAPR being smaller than a predefined threshold γ. Assume a signal $x(t)$ is obtained after the M-point IDFT in SC-FDMA or M-point IDFrFT in SC-SEFDMA, the PAPR calculation is therefore expressed as

$$PAPR = \frac{max|x(t)|^2}{E[|x(t)|^2]}, \tag{8}$$

where $max|x(t)|^2$ is the peak power of the signal $x(t)$, $E[.]$ is the expectation operator and $E[|x(t)|^2]$ indicates the average power.

Table I: Signal specifications

Parameter	SC-FDMA	SC-SEFDMA
Sampling frequency (MHz)	1.92	$1.92/\alpha$
M-point IFFT/FFT output sample length	128	128
N-point IFFT/FFT output sample length	12	12
No. of guard band sub-carriers	58	58
No. of data sub-carriers	12	12
Sub-carrier bandwidth (kHz)	15	$15/\alpha$
Bandwidth compression factor α	1	0.9, 0.8, 0.7
Sub-carrier spacing (kHz)	15	15
Total bandwidth (kHz)	180	180
Modulation scheme	QPSK	QPSK

Data rate improvement, using the non-orthogonal access strategy, is the performance criterion in this work. Therefore, we employ Type-II SEFDM waveforms for SC-SEFDMA. Signals, as configured in Table I, where one physical resource block (PRB) is tested with the sub-carrier bandwidth of 15 kHz for SC-FDMA and $15/\alpha$ kHz for SC-SEFDMA. It should be noted that the sub-carrier spacing for both signals is fitted at 15 kHz, which is the numerology defined in 5G NR [12]. As explained in Section II-B, either a single IFFT scheme or a multiple IFFT architecture is applicable for SEFDM signal generation. Therefore Table I uses parameters M/N-point IFFT/FFT for both SC-FDMA and SC-SEFDMA.

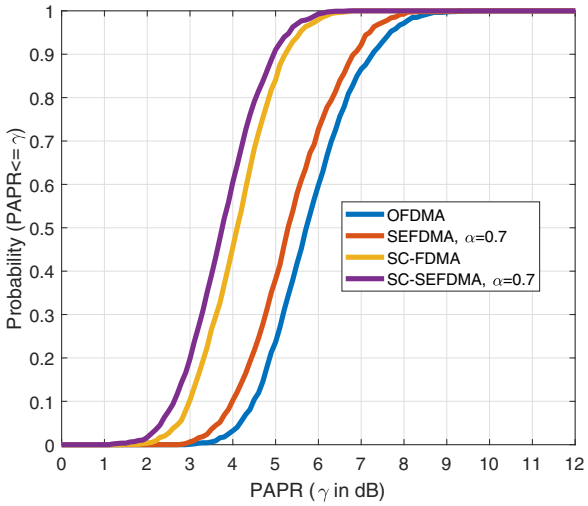

Fig. 3. PAPR comparison for single carrier and multicarrier access schemes.

Fig. 3 presents PAPR of four signals using the same number of sub-carriers. The PAPR values of traditional OFDMA and SEFDMA signals are calculated based on Table I but without the N-point IFFT/FFT operations. Results indicate that the probability of PAPR below and equal the threshold γ of SEFDMA is lower than that of OFDMA. With the single carrier operation included, PAPR is further reduced. It is worth mentioning that the SC-SEFDMA still has lower PAPR than SC-FDMA.

Channel coding is widely used in communication systems to mitigate channel effects and other impairments. LDPC [8] has been standardized for data channels of 5G NR [9] and later was proposed for non-orthogonal satellite communications [13]. Due to the 5G standard compatibility and the superior performance of LDPC, this work also applies LDPC coding for signal recovery. It should be noted that the rate matching for LDPC coding in this work depends on the redundancy version RV0 [9]. The LDPC decoder applies the belief propagation decoding algorithm [8] with 50 iterations for all the systems.

The advantages of SC-SEFDMA are studied from two perspectives; same data rate scenario and higher data rate scenario. In the first scenario, we configure the same effective data rate for both systems via tuning the bandwidth compression factor α and channel coding rate Rc. The effecitve data rate is computed as the following

$$R_e = Rc \times f_s \times log_2 O \times (N_d/N), \tag{9}$$

where R_e is the effective bit rate, f_s is sampling rate (e.g. f_s=1.92/α), O is constellation cardinality (e.g. O=4), N_d is

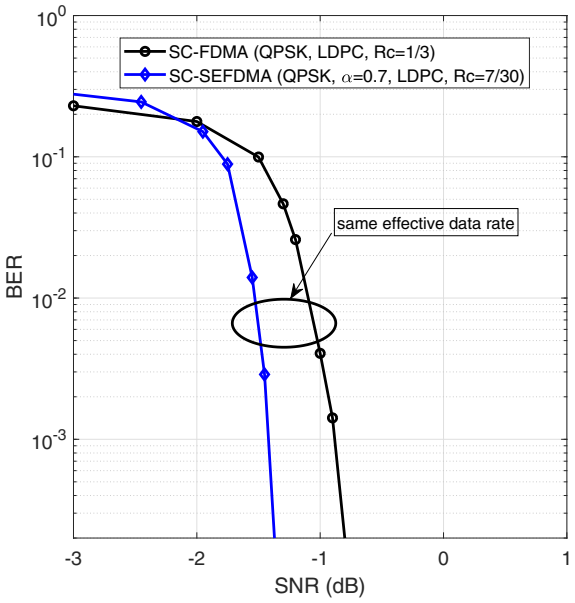

Fig. 4. BER comparison for systems at the same effective data rate.

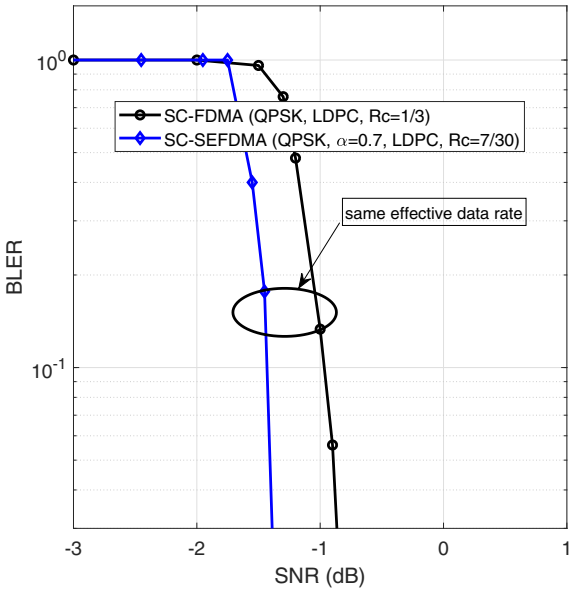

Fig. 5. BLER comparison for systems at the same effective data rate.

the number of data sub-carriers (e.g. N_d=12) and N is the number of total sub-carriers (N=128). For the case of two systems with equal data rates, QPSK modulated SC-SEFDMA at α=0.7 should be LDPC encoded with a rate Rc=7/30 while the QPSK modulated SC-FDMA is configured with coding rate Rc=1/3. Results in Fig. 4 indicate that achieving the same data rate, SC-SEFDMA can save 0.5 dB power compared with SC-FDMA. In addition to the bit error rate (BER) investigations in Fig. 4, block error rate (BLER) is obtained based on the 5G NR defined 24-bit cyclic redundancy check (CRC) [9] and is illustrated in Fig. 6 where the same advantage of 0.5 dB power saving is observed.

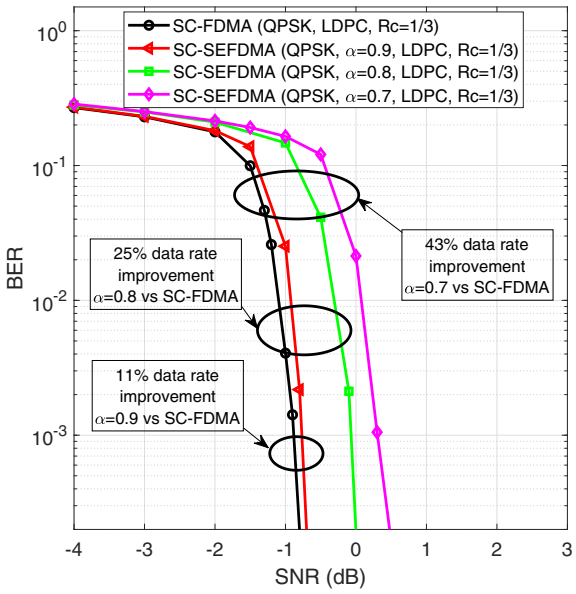

Fig. 6. BER comparison for systems at different effective data rate.

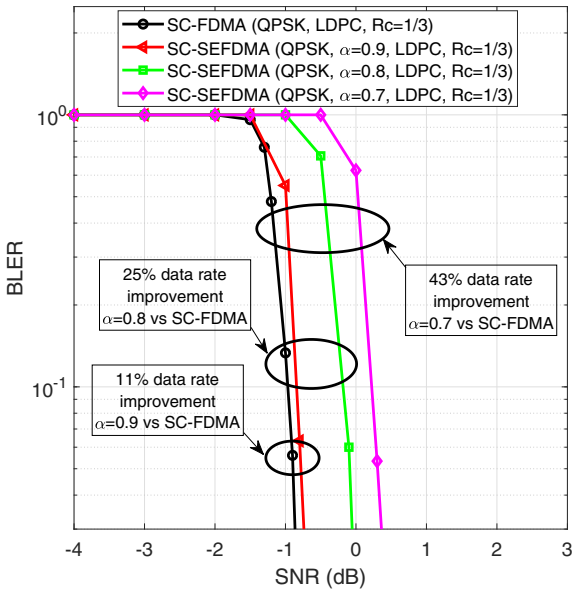

Fig. 7. BLER comparison for systems at different effective data rate.

We also evaluate systems at the same coding rate. In this case, SC-SEFDMA achieves higher data rate than that of SC-FDMA over the same signal bandwidth. For higher data rate scenarios, three different signals with α=0.9, 0.8

and 0.7 are evaluated and their performance is compared for BER and BLER in Fig. 6 and Fig. 7, respectively. Data rate improvement ratio is defined as

$$R_i = (\frac{1}{\alpha} - 1) \times 100\%. \quad (10)$$

Applying the SC-SEFDMA signal at α=0.7, data rate is improved by 43%. Unfortunately, due to the self-created ICI, system performance is compromised by 1.2 dB power degradation. Therefore, we could increase the value of α and thus mitigate the ICI at the cost of reducing data rate. With a higher α=0.8, which indicates 25% data rate improvement, the power degradation is reduced to 0.8 dB. Further increasing the α to 0.9, the power degradation is reduced to 0.1 dB but with the benefit of 11% data rate improvement.

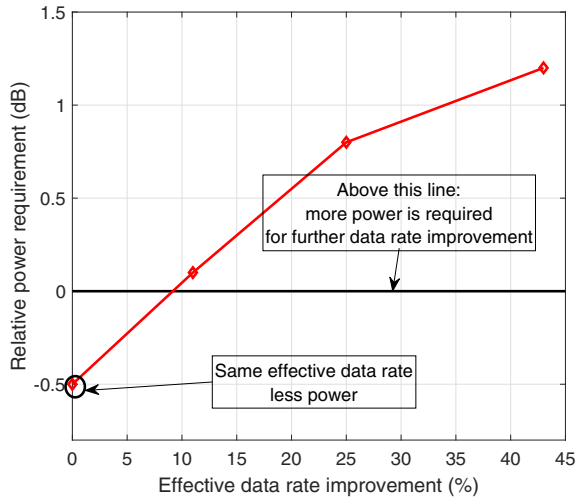

Fig. 8. Power requirement versus data rate improvement. Positive power indicates more power is required to reach the data rate and negative power means less power is required for a specific data rate.

To make the advantages of SC-SEFDMA more apparent, Fig. 8 shows the relationship of required power and data rate improvement by summarising the results of Fig. 4 and Fig. 6. A black solid horizontal line is the threshold to separate power penalty and power saving. The positive values above the threshold indicate the additional power required to reach a specific data rate, while the values below the threshold indicate less power is needed to reach a higher data rate. The correlation of power requirement and data rate improvement paves the way for the design of future spectrally efficient systems, for communications on uplink channels in wireless and mobile systems.

IV. Conclusion

A non-orthogonal single carrier access technique is proposed and verified, through simulations, in this work. Unlike orthogonal single carrier SC-FDMA, the proposed non-orthogonal single carrier access technique, termed SC-SEFDMA packs sub-carriers in a non-orthogonal format leading to improved spectral efficiency in either data rate improvement or spectral bandwidth resource saving. This work focuses on data rate improvement in SC-SEFDMA. The combination of the bandwidth compression factor α and the channel coding rate Rc determines the effective signal data rate. By properly tuning the two parameters, SC-SEFDMA can either save power at the same data rate as SC-FDMA or achieve higher data rate than SC-FDMA.

This work also reveals that, considering the same channel coding rate, to achieve a data rate improvement higher than a threshold, SC-SEFDMA requires extra power budget. A possible solution of cutting the extra power consumption is to design interference cancellation strategies for SC-SEFDMA signals prior to the LDPC decoding. In this case, the efficiency of using LDPC code is maximized. Another possible option is to evaluate higher order modulation formats. The joint consideration of bandwidth compression factor, channel coding rate and modulation scheme would lead to a more efficient SC-SEFDMA design.

References

[1] H. Holma and A. Toskala, *LTE for UMTS: OFDMA and SC-FDMA Based Radio Access*. John Wiley & Sons Ltd, 2009.

[2] H. G. Myung, J. Lim, and D. J. Goodman, "Single carrier FDMA for uplink wireless transmission," *IEEE Vehicular Technology Magazine*, vol. 1, no. 3, pp. 30–38, Sep. 2006.

[3] G. Berardinelli, L. A. M. Ruiz de Temino, S. Frattasi, M. I. Rahman, and P. Mogensen, "OFDMA vs. SC-FDMA: performance comparison in local area IMT-A scenarios," *IEEE Wireless Communications*, vol. 15, no. 5, pp. 64–72, Oct. 2008.

[4] I. Darwazeh, H. Ghannam, and T. Xu, "The first 15 years of SEFDM: A brief survey," in *11th International Symposium on Communication Systems, Networks Digital Signal Processing (CSNDSP18)*, Jul. 2018, pp. 1–7.

[5] I. Kanaras, A. Chorti, M. Rodrigues, and I. Darwazeh, "A fast constrained sphere decoder for ill conditioned communication systems," *Communications Letters, IEEE*, vol. 14, no. 11, pp. 999–1001, Nov. 2010.

[6] T. Xu, R. C. Grammenos, F. Marvasti, and I. Darwazeh, "An improved fixed sphere decoder employing soft decision for the detection of non-orthogonal signals," *IEEE Communications Letters*, vol. 17, no. 10, pp. 1964–1967, Oct. 2013.

[7] T. Xu, T. Xu, and I. Darwazeh, "Deep learning for interference cancellation in non-orthogonal signal based optical communication systems," in *2018 Progress In Electromagnetics Research Symposium - Spring (PIERS)*, Aug. 2018 (invited), pp. 241–248.

[8] R. G. Gallager, *Low-Density Parity-Check Codes*. MIT Press, 1963.

[9] 3GPP TS 38.212 version 15.2.0 Release 15, "5G NR; multiplexing and channel coding," Rel. 15, Jul. 2018.

[10] T. Xu and I. Darwazeh, "Transmission experiment of bandwidth compressed carrier aggregation in a realistic fading channel," *IEEE Transactions on Vehicular Technology*, vol. 66, no. 5, pp. 4087–4097, May 2017.

[11] D. H. Bailey and P. N. Swarztrauber, "The fractional fourier transform and applications," *SIAM Review*, vol. 33, no. 10, pp. 389–404, 1991.

[12] E. Dahlman, S. Parkvall, and J. Sköld, *5G NR: The Next Generation Wireless Access Technology*. Academic Press, 2018.

[13] H. Ghannam and I. Darwazeh, "SEFDM over satellite systems with advanced interference cancellation," *IET Communications*, vol. 12, no. 1, pp. 59–66, 2018.